ADVANCES IN ATMOSPHERIC SCIENCES, VOL. 30, NO. 1, 2013, 48–56

Relationship between Bering Sea Ice Cover and East Asian Winter Monsoon Year-to-Year Variations

LI Fei*[1,3] (李 菲) and WANG Huijun[1,2] (王会军)

[1] *Nansen-Zhu International Research Center, Institute of Atmospheric Physics, Chinese Academy of Sciences, Beijing* 100029

[2] *Climate Change Research Center, Chinese Academy of Sciences, Beijing* 100029

[3] *University of Chinese Academy of Sciences, Beijing* 100049

(Received 11 April 2012; revised 17 May 2012)

ABSTRACT

In this study, the relationship between year-to-year variations in the Bering Sea ice cover (BSIC) and the East Asian winter monsoon (EAWM) for the period 1969–2001 was documented. The time series of total ice cover in the eastern Bering Sea correlated with the EAWM index at −0.49, indicating that they are two tightly related components. Our results show that the BSIC was closely associated with the simultaneous local and large-scale atmosphere over the Asian–northern Pacific region. Heavy BSIC corresponded to weaker EAWM circulations and light BSIC corresponded to stronger EAWM circulations. Thus, the BSIC should be considered as one of the possible factors affecting the EAWM variation.

Key words: Bering Sea ice cover, East Asian winter monsoon, year-to-year variation

Citation: Li, F., and H. J. Wang, 2013: Relationship between Bering Sea ice cover and East Asian winter monsoon year-to-year variations. *Adv. Atmos. Sci.*, **30**(1), 48–56, doi: 10.1007/s00376-012-2071-2.

1. Introduction

The East Asian winter monsoon (EAWM) is one of the most active atmospheric circulation systems in boreal winter. It can exert strong impacts on local weather and climate over East Asia and the northwestern Pacific (Ding and Krishnamurti, 1987; Ding, 1990; Zhang et al., 1997; Compo et al., 1999; Sun et al., 2009; Wang et al., 2011). In the past, interest in EAWM research has been boosted by the increase in the frequency and severity of weather-related disasters in China that result from anomalous EAWMs. Particularly in January and early February 2008, an anomalously strong EAWM occurred with extremely low regional temperatures, blizzard conditions in northern China, and freezing rain in southern China (Wang and Jiang, 2004; Zhou et al., 2009; Han et al., 2011). Previous studies have shown that factors influencing the EAWM include El Niño-Southern Oscillation (ENSO; Li, 1990; Tomita and Yasunari, 1996; Wang et al., 2000; Wang and Zhang, 2002), North Atlantic Oscillation (NAO; Wu et al., 1999), and Arctic Oscillation (AO; Gong et al., 2001; Wu and Wang, 2002a, b; Wang and Sun, 2009), as well as conditions on the Tibetan Plateau and Eurasian snow cover (Walland and Simmonds, 1996; Watanabe and Nitta, 1999).

Arctic sea ice is a critical component of the climate system, influenced by both the atmosphere and ocean. Variations in Arctic sea ice cover may modulate local climate through the ice albedo feedback, the insulating effect, deep water formation, and freshwater budget (Walsh, 1983; Barry et al., 1993; Curry et al., 1995), and at middle and high latitudes it can be manifested as altered patterns of atmospheric circulation and precipitation (Overland and Pease, 1982; Parkinson, 1990; Agnew, 1993; Slonosky et al., 1997; Prinsenberg et al., 1997; Wu et al., 1999, Serreze et al., 2007; Wang and Zhang, 2010; Ma et al., 2012). Wu et al. (2011) explored the relation between the autumn–winter Arctic sea ice and the winter Siberian High. Liu et al. (2007) investigated two dominant modes of the North Pacific sea ice variability and their association

*Corresponding author: LI Fei, lifei-715@163.com

with East Asian–northern Pacific winter climate. Recently, Liu et al. (2012) demonstrated that the decline of the autumn sea ice cover in the Arctic is a precursor of winter snowfall.

Although it is known that the EAWM is linked to Arctic sea ice cover, some uncertainty remains. The purposes of this study were to identify the key regions in which sea ice significantly related to winter climate over East Asia and to advance our understanding of the causes of EAWM year-to-year variations.

2. Datasets

The Arctic sea ice concentration data (1°×1° grid resolution) for the period 1980–2010 were obtained from the UK Meteorological Office as the Hadley Centre sea ice and sea surface temperature dataset version 1 (HadISST1; Rayner et al., 2003). The monthly mean atmospheric data (2.5°×2.5° grid resolution) was obtained from the National Centers for Environmental Prediction–National Center for Atmospheric Research (NCEP–NCAR) Global Reanalysis 1 (NCEP-1; Kalnay et al., 1996). The variables included sea level pressure (SLP), surface air temperature (SAT), 850-hPa wind vector (UV850), 500-hPa geopotential height (HGT500), and 200-hPa zonal wind (U200). In this study, sea ice cover refers to the actual area covered by sea ice with 15% and greater ice concentration. The winter of 1969 refers to the 1969/1970 winter. The months of December, January, and February were used to calculate the winter mean for all variables (e.g., sea ice and atmosphere).

3. The key region of sea ice variability

Figure 1 shows the spatial pattern of the standard deviation of the wintertime Arctic sea ice cover for the period 1969–2001. Large interannual variability was confined to a rather narrow belt along the climatologic mean ice edges, including the Greenland and Barents Seas and the Davis Strait in the Atlantic sector and the Bering Sea and the Sea of Okhotsk in the Pacific sector, consistent with previous studies (Walsh and Johnson, 1979; Fang and Wallace, 1994; Deser, 2000). Parkinson et al. (1999) also indicated that all of these areas were seasonally ice impacted. In the Atlantic sector the most rapid growth occurred in autumn (September–November) and continued throughout the winter, whereas in the Pacific sector the most rapid growth occurred in late autumn and earlier winter (November–January).

The correlation coefficient of the wintertime Arctic sea ice cover with the EAWM index was calculated to identify the regions of interest (Fig. 2a). Here we used

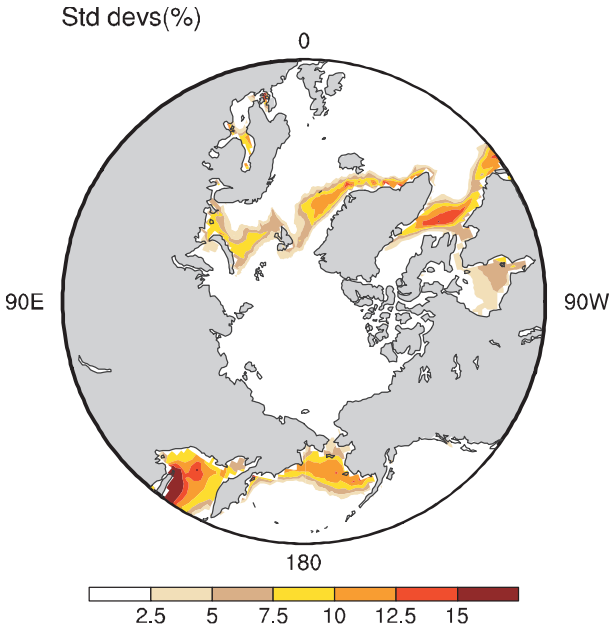

Fig. 1. Standard deviations (%) of the wintertime (December–February) Arctic sea ice cover for the period 1969–2001.

an EAWM index defined as the first the empirical orthogonal function (EOF) mode of 850-hPa air temperature within the EAWM domain (20°–60°N, 90°–150°E) (Li and Wang, 2012). A high negative correlation area over the eastern Bering Sea (55°–66°N, 160°–180°W) is obvious in this figure, with a peak value of −0.67 (statistically significant at $p<0.01$). This result indicates that the eastern Bering Sea is a key region in which sea ice is significantly related to the East Asian winter climate. In addition, the simultaneous rapid ice growth in the Pacific sector shows a closer relation to the EWAM.

Figure 2b displays the time series of total ice cover in the eastern Bering Sea, in this study defined as the Bering Sea ice cover (BSIC) index, together with the EAWM index. The BSIC index varies on strong interannual and interdecadal timescales and was out of phase with the EAWM index. The BSIC and the EAWM correlated at −0.49 (statistically significant at $p<0.05$), indicating that they are two closely related components.

4. The BSIC–EAWM connection

We then analyzed the simultaneous atmospheric circulation anomalies associated with the BSIC over the Asian–northern Pacific region, and two types of analyses were performed: a composite analysis and a linear regression analysis. According to the time series of the total ice cover in the eastern Bering Sea

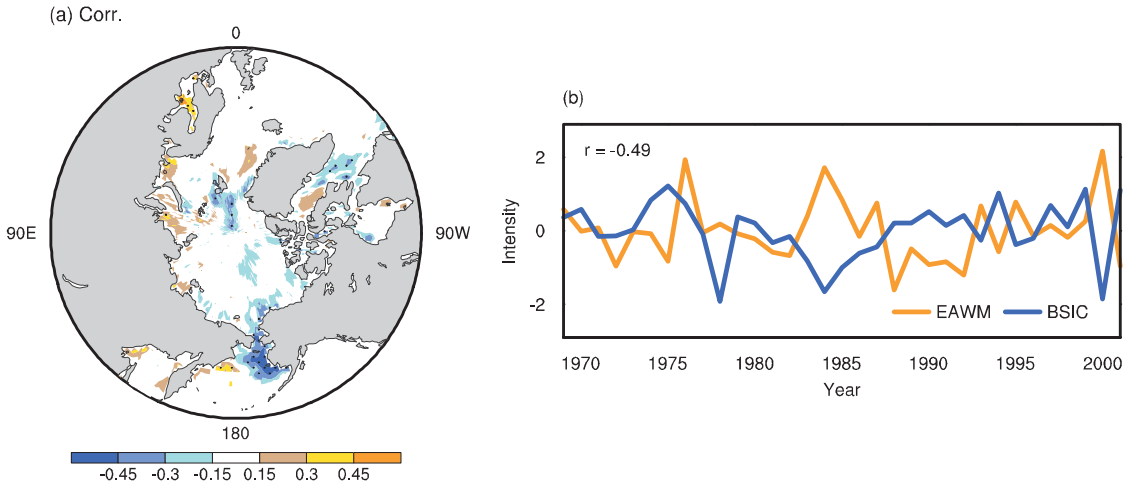

Fig. 2. (a) Correlation coefficients of the wintertime (December–February) Arctic sea ice cover with the EAWM index for the period 1969–2001, after removing the linear trend. According to a Student's t-test, dotted areas indicate correlations that exceed the $p<0.05$ significance level. (b) Time series of total ice cover (10^5 km^2) in the eastern Bering Sea (55°–66°N, 160°–180°W), together with the EAWM index, after removing the linear trend.

(Fig. 2b), we selected heavy and light BSIC cases based on the absolute and normalized values of the BSIC index >1.0 standard deviation. Thus, the heavy BSIC cases included 1975, 1994, 1999, and 2001; the light BSIC cases included 1978, 1984, 1985, and 2000. Figure 3 shows the composite differences of atmospheric circulation anomalies during heavy ice years. At the surface, an increase in SLP was located in the Kamchatka peninsula and the western Bering Sea, near the climatological center for the Aleutian low, and a reduction occurred to the east over Alaska (Fig. 3a). The positive signs and maximum increase above 3 hPa appeared to be related to a weaker Aleutian Low that moved westward of normal.

Figure 3b shows positive values of SAT over northern Asia, East Asia, and the northwestern Pacific, and negative values to the east over the Bering Sea. The negative signs increased sharply in amplitude, and the maximum dropped below −4°C. These results can be explained by the local sea ice amplification as well as the large-scale wind anomalies at 850 hPa (Fig. 3c). An ice advance in the eastern Bering Sea was followed by a strengthening of the circumpolar westerly that moved down over the Bering region. Besides, it exhibited strong anticyclonic vorticities with a weakening of the midlatitude westerly between 80°E and the dateline. East of the anticyclonic vorticities, anomalous northerly and northwesterly winds over the Bering region favored negative SLP anomalies and colder conditions in that region by colder air transported from the north. Southwest of the anticyclonic vorticities, anomalous easterly and southeasterly winds over the northwestern Pacific and East Asia suggested weaker northeasterly monsoonal flow and favored warmer conditions in that region by warmer and wetter air transported from the ocean.

At 500 hPa, an elongated increase was observed over northern Asia and the Sea of Okhotsk, with a major ridge extending southeastward along the East Asian coast. Besides, a reduction was observed to the east over the eastern Bering Sea and Alaska. This spatial pattern suggested both a weakened East Asian trough and a western ridge over North America, and in the vertical direction it featured a barotropic structure. At 200 hPa, anomalous easterly winds prevailed south of Lake Baikal west of the dateline, with anomalous westerly winds to the north (Fig. 3e), indicating a weakening and retreat of the East Asian jet.

In contrast, Fig. 4 shows the composite differences of atmospheric circulation anomalies during light ice years. At the surface, a decrease in SLP occurred in the Bering Sea, and the maximum dropped below −4 hPa (Fig. 4a). This implies that a deeper Aleutian Low had moved eastward of normal. Figure 4b shows negative values of SAT over northern Asia, the Sea of Okhotsk, and the northwestern Pacific, and positive values are evident to the east over the Bering Sea and Alaska, with a maximum >6°C. At 850 hPa, an ice retreat in the eastern Bering Sea was accompanied by a weakening of the circumpolar westerly that exhibited strong cyclonic vorticities over the Bering Sea region and a strengthening of the midlatitude westerly

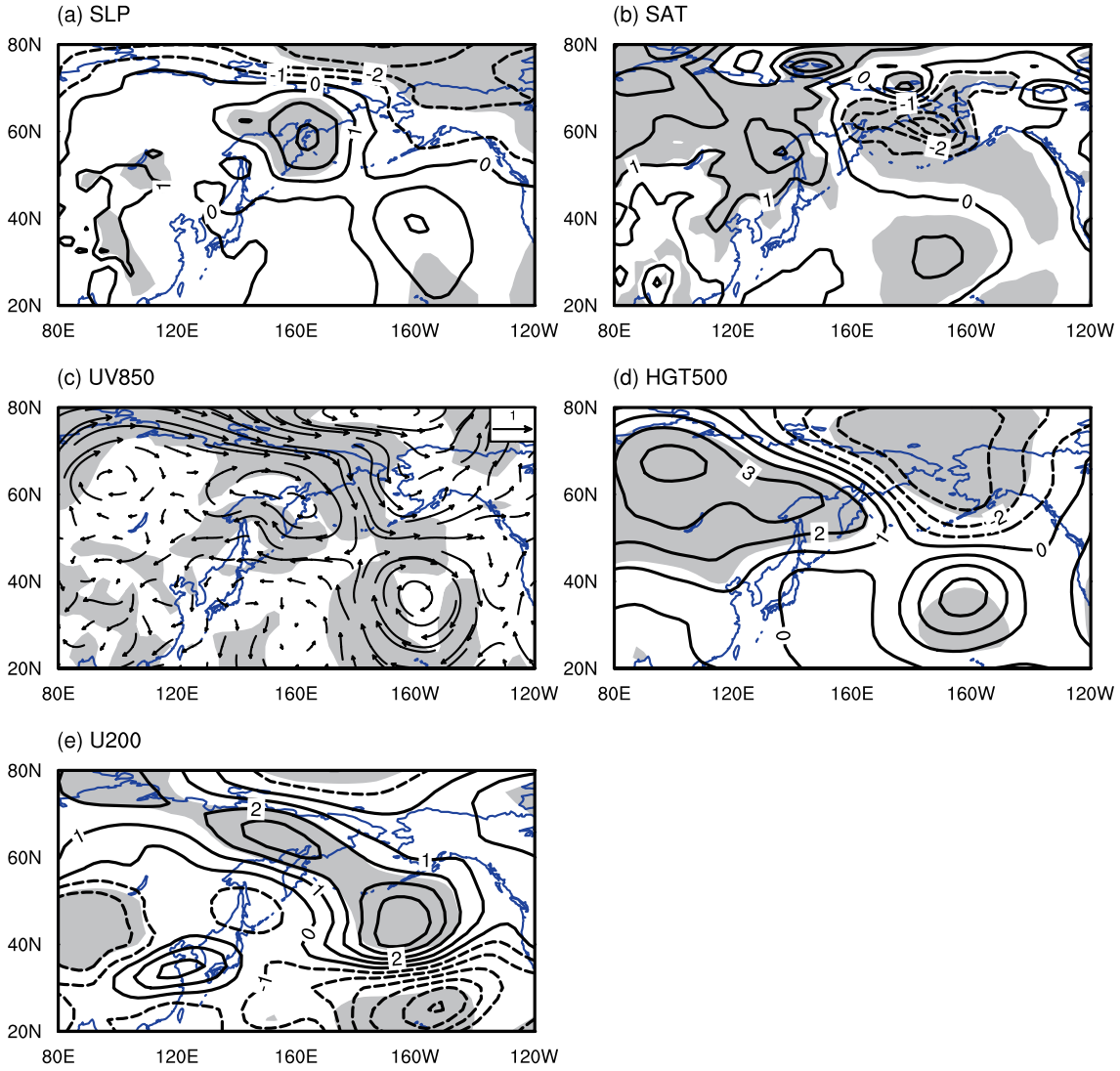

Fig. 3. Composite differences of atmospheric circulation anomalies during heavy ice years, in terms of (a) SLP (units: hPa), (b) SAT (units: °C), (c) UV850 (units: m s^{-1}), (d) HGT500 (units: gpm), and (e) U200 (units: m s^{-1}). According to a Student's t-test, shaded areas indicate correlations that exceed the $p < 0.05$ significance level.

between 80°E and 150°W (Fig. 4c). East of the cyclonic vorticities, anomalous southerly and southeasterly winds over the eastern Bering Sea favored positive SLP anomalies and warmer conditions in that region by warmer and wetter air transported from the ocean. Southwest of the cyclonic vorticities, anomalous northeasterly winds over northern Asia suggested stronger northeasterly monsoonal flow and favored colder conditions in that region by colder air transported from the north.

At 500 hPa, an elongated decrease occurred over northern Asia, the Sea of Okhotsk, and the western Bering Sea, and an increase occurred to the east over Alaska and the Gulf of Alaska (Fig. 4d). This spatial pattern suggests both a strengthened East Asian trough and a western ridge over North America, and in the vertical direction it featured a barotropic structure. At 200 hPa, anomalous westerly winds prevailed south of Lake Baikal west of the dateline, with anomalous easterly winds to the north (Fig. 4e), indicating the strengthening and advance of the East Asian jet.

In summary, the results shown in Figs. 3 and 4 indicate that the BSIC is closely associated with the simultaneous local and large-scale atmosphere over the Asian–northern Pacific region. The characteristics of the composite differences during heavy and light ice years largely mirror each other. Heavy BSIC corresponds to a weaker Aleutian Low that has westward

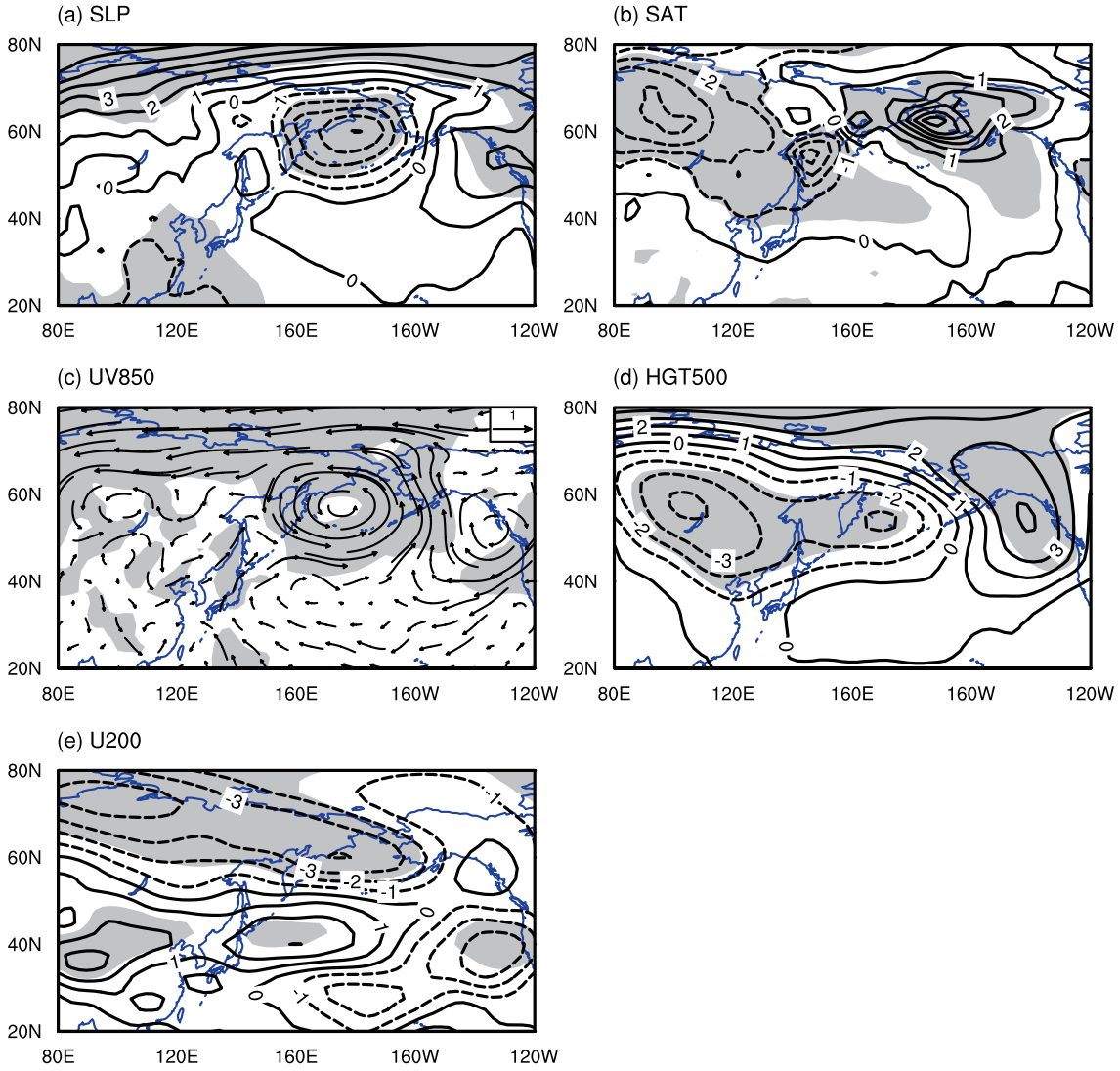

Fig. 4. Same as Fig. 3, but for light ice years.

moved and light BSIC corresponds to a deeper Aleutian Low that has eastward moved, as well as other features, in the following aspects: northeasterly monsoonal flow over East Asia, East Asian trough and western ridge over North America at 500 hPa, and East Asian jet at 200 hPa.

Figure 5 shows the regression coefficients of atmospheric circulation anomalies with regression on the BSIC index. Corresponding to heavy ice years, an increase in SLP occurred in eastern Siberia and the western Bering Sea, and the maximum exceeded 2 hPa (Fig. 5a). Figure 5b shows positive values of SAT over northern Asia and the Sea of Okhotsk and negative values to the east over the Bering Sea. At 850 hPa, the structure was characterized by a strengthening of the circumpolar westerly that moved down over the eastern Bering Sea. Besides, it exhibited strong anticyclonic vorticities with a weakening of the midlatitude westerly between 80°E and 160°W (Fig. 3c).

At 500 hPa, an increase occurred over northern Asia and the Sea of Okhotsk, with a major ridge extending southeastward along the East Asian coast, and a decrease to the east over Alaska. At 200 hPa, anomalous easterly winds prevailed south of Lake Baikal west of the dateline, with anomalous westerly winds to the north (Fig. 4e).

For comparison, we also present the regression coefficients of atmospheric circulation anomalies with regression on the EAWM index (Fig. 6). Corresponding to weak monsoon events, an increase in SLP occurred in the northern Pacific and the Bering Sea (Fig. 6a), consistent with the BSIC-regressed SLP except for

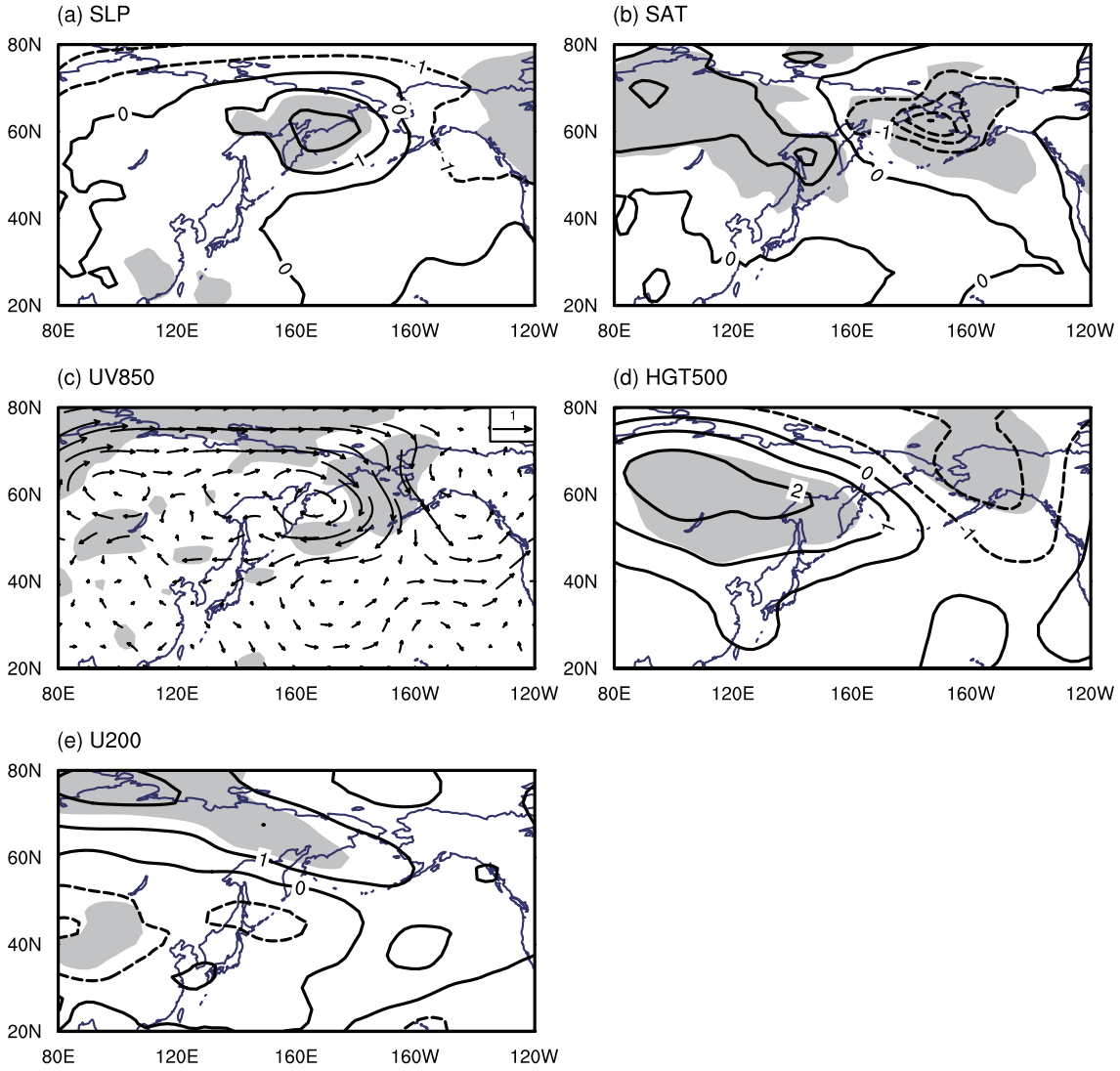

Fig. 5. Regression coefficients of wintertime (December–February) atmospheric circulation anomalies with regression on the BSIC index, in terms of (a) SLP (units: hPa), (b) SAT (units: °C), (c) UV850 (units: m s^{-1}), (d) HGT500 (units: gpm), and (e) U200 (units: m s^{-1}), after removing the linear trend. According to a Student's t-test, shaded areas indicate correlations that exceed the $p < 0.05$ significance level.

a southeastward shift. Figures 6b–e display similar southeastward shifts in the northern Pacific.

Figure 6b shows positive values of SAT over the entirety of Asia and the northwestern Pacific, and negative values are shown to the east over Alaska. At 850 hPa, a strengthening of the circumpolar westerly moved down over the eastern Bering Sea and Gulf of Alaska and exhibited strong anticyclonic vorticities, and a weakening of the midlatitude westerly occurred between 80°E and 140°W (Fig. 6c). At 500 hPa, an increase extended from Lake Baikal eastward toward the northeastern Pacific (Fig. 6d). At 200 hPa, anomalous easterly winds prevailed south of Lake Baikal between 80°E and 140°W, with anomalous westerly winds to the north (Fig. 6e).

Overall, in the regression maps with regression on both the BSIC and EAWM index (Figs. 5 and 6), characteristics of all cases were in good agreement with those in the composite maps (Fig. 3). However, the EAWM-regressed anomalies were more apparent and showed significant southeastward shifts in the northern Pacific.

5. Discussion and conclusions

The EAWM is one of the most active systems in boreal winter and is linked to the behavior of many factors (i.e., ENSO, NAO, and AO, as well as conditions

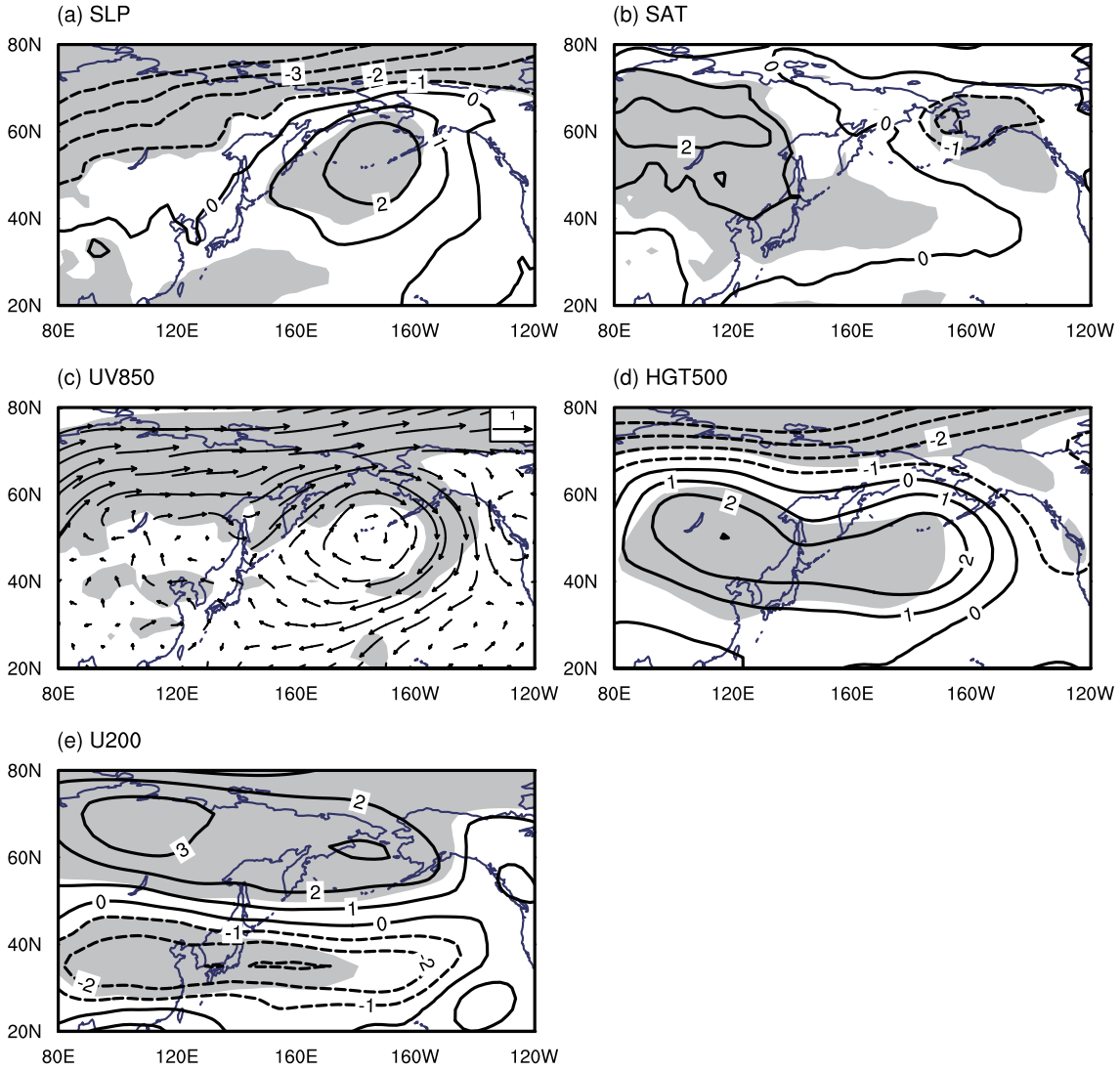

Fig. 6. Same as Fig. 5, but for regression on the EAWM index.

on the Tibetan Plateau and Eurasian snow cover). By analyzing the connection between the EAWM and the entire Arctic sea ice cover, we identified a key region in which sea ice significantly related to the East Asian winter climate. The time series of the total ice cover in the eastern Bering Sea correlated with the EAWM index at −0.49, indicating that they are two closely related components.

Our results indicate that BSIC is closely associated with the simultaneous local and large-scale atmosphere over the Asian–northern Pacific region. We used two types of analyses: a linear regression analysis and a composite analysis. Heavy BSIC corresponds to a weaker Aleutian Low that has moved westward of normal and light BSIC corresponds to a deeper Aleutian Low that has moved eastward of normal, as well as other features, in the following aspects: monsoonal flow over East Asia, East Asian trough and western ridge over North America at 500 hPa, and East Asian jet at 200 hPa.

In addition, the relationship between BSIC and EAWM is not stationary. It undergoes interannual variability as well as interdecadal shifts. A detailed understanding of ice–atmosphere interactions is a necessary pursuit for further investigation.

Acknowledgements. This work was supported by the National Natural Science Foundation of China (Grant No. 41130103), the Chinese Academy of Sciences Innovation Key Program (Grant No. KZCX2-YW-QN202), and the Major State Basic Research Development Program of China 973 Program (Grant No. 2009CB421406).

REFERENCES

Agnew, T., 1993: Simultaneous winter sea-ice and atmospheric circulation anomaly patterns. *Atmos.–Ocean,* **31**(2), 259–280.

Barry, R. G., M. C. Serreze, J. A. Maslanik, and R. H. Preller, 1993: The Arctic sea-ice climate system: Observations and modeling. *Rev. Geophys.,* **31**(4), 397–422.

Compo, G. P., G. N. Kiladis, and P. J. Webster, 1999: The horizontal and vertical structure of east Asian winter monsoon pressure surges. *Quart. J. Roy. Meteor. Soc.,* **125**(553), 29–54.

Curry, J. A., J. L. Schramm, and E. E. Ebert, 1995: Sea ice-albedo climate feedback mechanism. *J. Climate,* **8**(2), 240–247.

Deser, C., 2000: On the teleconnectivity of the Arctic Oscillation. *Geophys. Res. Lett.,* **27**(6), 779–782.

Ding, Y. H., 1990: Build-up, air mass transformation and propagation of Siberian high and its relation to cold surge in east Asia. *Meteor. Atmos. Phys.,* **44**, 281–292.

Ding, Y. H., and T. N. Krishnamurti, 1987: Heat budget of the Siberian high and the winter monsoon. *Mon. Wea. Rev.,* **115**, 2428–2449.

Fang, Z., and J. M. Wallace, 1994: Arctic sea ice variability on a timescale of weeks and its relation to atmospheric forcing. *J. Climate,* **7**(12), 1897–1914.

Gong, D. Y., S. W. Wang, and J. H. Zhu, 2001: East Asian winter monsoon and Arctic Oscillation. *Geophys. Res. Lett.,* **28**(10), 2073–2076.

Han, Z., S. L. Li, and M. Mu, 2011: The role of warm North Atlantic SST in the formation of positive height anomalies over the Ural Mountains during January 2008. *Adv. Atmos. Sci.*, **28**(2), 246–256, doi: 10.1007/s00376-010-0069-1.

Kalnay, E., and Coauthors, 1996: The NCEP/NCAR 40-year reanalysis project. *Bull. Amer. Meteor. Soc.,* **77**(3), 437–471.

Li, C. Y., 1990: Interaction between anomalous winter monsoon in East Asia and El Niño events. *Adv. Atmos. Sci.*, **7**(1), 36–46.

Li, F., and H. J. Wang, 2012: Predictability of the East Asian winter monsoon interannual variability as indicated by the DEMETER CGCMS. *Adv. Atmos. Sci.*, **29**(3), 441–454.

Liu, J. P., Z. H. Zhang, R. M. Horton, C. Y. Wang, and X. B. Ren, 2007: Variability of north Pacific sea ice and East Asia–North Pacific winter climate. *J. Climate*, **20**(10), 1991–2001.

Liu, J. P., J. A. Curry, H. J. Wang, M. R. Song, and R. M. Horton, 2012: Impact of declining Arctic sea ice on winter snowfall. *Proc. Natl. Acad. Sci. USA,* **109**(11), 4074–4079.

Ma, J. H., H. J. Wang, and Y. Zhang, 2012: Will boreal winter precipitation over China increase in the future? An AGCM simulation under summer "ice-free Arctic" conditions. *Chinese Science Bulletin,* **57**(8), 921–926.

Overland, J. E., and C. H. Pease, 1982: Cyclone climatology of the Bering Sea and its relation to sea ice extent. *Mon. Wea. Rev.,* **110**(1), 5–13.

Parkinson, C. L., 1990: The impacts of the Siberian high and Aleutian low on the sea-ice cover of the Sea of Okhotsk. *Annals of Glaciology,* **14**, 226–229.

Parkinson, C. L., D. J. Cavalieri, P. Gloersen, H. J. Zwally, and J. C. Comiso, 1999: Arctic sea ice extents, areas, and trends, 1978–1996. *J. Geophys. Res.,* **104**(C9), 20837–20856.

Prinsenberg, S. J., I. K. Peterson, S. Narayanan, and J. U. Umoh, 1997: Interaction between atmosphere, ice cover, and ocean off Labrador and Newfoundland from 1962–1992. *Canadian Journal of Fisheries and Aquatic Sciences,* **54**(S1), 30–39.

Rayner, N. A., D. E. Parker, E. B. Horton, C. K. Folland, L. V. Alexander, D. P. Rowell, E. C. Kent, and A. Kaplan, 2003: Global analyses of sea surface temperature, sea ice, and night marine air temperature since the late nineteenth century. *J. Geophys. Res.,* **108**, doi: 10.1029/2002JD002670.

Serreze, M. C., M. M. Holland, and J. Stroeve, 2007: Perspectives on the Arctic's shrinking sea-ice cover. *Science,* **315**(5818), 1533–1536.

Slonosky, V. C., L. A. Mysak, and J. Derome, 1997: Linking Arctic sea-ice and atmospheric circulation anomalies on interannual and decadal timescales. *Atmos.–Ocean,* **35**(3), 333–366.

Sun J. Q., H. J. Wang, and W. Yuan, 2009: A preliminary investigation on causes of the catastrophic snowstorm in March, 2007 in northeastern part of China. *Acta Meteorologica Sinica,* **67**(3), 469–477.

Tomita, T., and T. Yasunari, 1996: Role of the northeast winter monsoon on the biennial oscillation of the ENSO/monsoon system. *J. Meteor. Soc. Japan,* **74**(4), 399–413.

Walland, D. J., and I. Simmonds, 1996: Modelled atmospheric response to changes in Northern Hemisphere snow cover. *Climate Dyn.,* **13**(1), 25–34.

Walsh, J. E. 1983: The role of sea ice in climatic variability: Theories and evidence. *Atmos.–Ocean,* **21**(3), 229–242.

Walsh, J. E., and C. M. Johnson, 1979: An analysis of Arctic sea ice fluctuations, 1953–77. *J. Phys. Oceanogr.,* **9**, 580–591.

Wang, B., and Q. Zhang, 2002: Pacific–East Asian teleconnection. Part II: How the Philippine Sea anomalous anticyclone is established during El Niño development. *J. Climate,* **15**(22), 3252–3265.

Wang, B., R. G. Wu, and X. H. Fu, 2000: Pacific–East Asian teleconnection: How does ENSO affect East Asian climate? *J. Climate,* **13**(9), 1517–1536.

Wang, H. J., and D. B. Jiang, 2004: A new East Asian winter monsoon intensity index and atmospheric circulation comparison between strong and weak composite. *Quaternary Sciences,* **24**(1), 19–27. (in Chinese)

Wang, H. J., and J. Q. Sun, 2009: Variability of Northeast China river break-up date. *Adv. Atmos. Sci.*, **26**(4),

701–706, doi: 10.1007/s00376-009-9035-1.

Wang, H. J., and Y. Zhang, 2010: Model projections of East Asian summer climate under the "free Arctic" scenario. *Atmos. Oceanic Sci. Lett.*, **3**(3), 176–180.

Wang, H. J., E. T. Yu, and S. Yang, 2011: An exceptionally heavy snowfall in Northeast China: Large-scale circulation anomalies and hindcast of the NCAR WRF model. *Meteor. Atmos. Phys.,* **113**, 11–25.

Watanabe, M., and T. Nitta, 1999: Decadal changes in the atmospheric circulation and associated surface climate variations in the Northern Hemispheric winter. *J. Climate,* **12**(2), 494–510.

Wu, B. Y., and R. H. Huang, 1999: Effects of the extremes in the North Atlantic Oscillation on East Asia winter monsoon. *J. Atmos. Sci.,* **23**, 641–651. (in Chinese)

Wu, B. Y., and J. Wang, 2002a: Possible impacts of winter Arctic Oscillation on Siberian high, the East Asian winter monsoon and sea-ice extent. *Adv. Atmos. Sci.,* **19**(2), 297–320.

Wu, B. Y., and J. Wang, 2002b: Winter Arctic Oscillation, Siberian high and East Asian winter monsoon. *Geophys. Res. Lett.,* **29**(19), doi: 10.1029/2002GL015373.

Wu, B. Y., R. H. Huang, and D. Y. Gao, 1999: Impact of variations of winter sea-ice extents in the Kara/Barents Seas on winter monsoon over East Asia. *Acta Meteorologica Sinica,* **13**, 141–153.

Wu, B. Y., J. Z. Su, and R. H. Zhang, 2011: Effects of autumn–winter Arctic sea ice on winter Siberian high. *Chinese Science Bulletin,* **56**(30), 3220–3228.

Zhang, Y., K. R. Sperber, and J. S. Boyle, 1997: Climatology and interannual variation of the East Asian winter monsoon: Results from the 1979–95 NCEP/NCAR reanalysis. *Mon. Wea. Rev.,* **125**(10), 2605–2619.

Zhou, W., J. C. L. Chan, W. Chen, J. Ling, J. G. Pinto, and Y. P. Shao, 2009: Synoptic-scale controls of persistent low temperature and icy weather over southern China in January 2008. *Mon. Wea. Rev.,* **137**(11), 3978–3991.